J. Electroanal. Chem., 75 (1977) 487—505

THE ELECTROCHEMISTRY OF PROTEINS AND RELATED SUBSTANCES

I. CYSTINE AND CYSTEINE AT THE MERCURY ELECTRODE *

MARIAN T. STANKOVICH and ALLEN J. BARD

Department of Chemistry, The University of Texas at Austin, Austin, Texas 78712 (U.S.A.)

(Received 19th May 1976)

ABSTRACT

Studies of the electroreduction of cystine (RSSR) and oxidation of cysteine (RSH) at several pH's at a hanging Hg drop electrode by cyclic voltammetry and at a Hg pool by coulometry are described. The proposed mechanism for RSSR involves reduction of an adsorbed monolayer (maximum coverage of 41 μC cm^{-2}) to form solution phase RSH at the adsorption prewave. A diffusion controlled reduction of RSSR to RSH occurs at more negative potentials. Oxidation of RSH involves formation of an adsorbed organomercury species, e.g., $Hg(RS)_2$ (maximum coverage of 80 μC cm^{-2}), which is reducible back to RSH. At higher RSH concentrations, anodic and cathodic current spikes appear on the cyclic voltammograms which are ascribed to formation of a tight or compact film when monolayer coverage of $Hg(RS)_2$ is attained, corresponding to strong interactions between adsorbed species.

INTRODUCTION

Substances containing the disulfide bond (—S—S—) adsorb strongly at the mercury electrode. Thus in studies of proteins in vitro or in the attempted analysis of whole blood, blood plasma, or other biological fluids, coverage of the electrode with protein, even from solutions as dilute as 10^{-7} *M* in protein, is frequently observed. While the electrochemical behavior of the protein itself may be of interest, this strong adsorption often leads to blockage of the electrode for other electrode reactions and may be a hindrance to the application of electrochemical techniques to in vivo analysis. On the other hand, this strong adsorption may be applicable to the modification of the electrode surface. There has recently been much interest in the "chemical modification" [1] of electrode surfaces (e.g., SnO_2, carbon) by the covalent bonding of molecules to the surface using, for example, organosilane reagents, so as to prepare "derivatized" electrodes with new and useful properties [1—3]. Strong irreversible adsorption, such as observed for allyl compounds at Pt electrodes

* In honour of Dr. G.C. Barker's 60th birthday.

[4], can also serve as a means of modifying the surface. Thus the strong adsorption of proteins, including enzymes and other potentially useful species, may lead to interesting types of electrodes. In this connection it is important to know the structural and conformational stability of the adsorbed molecule and the changes that occur upon electroreduction or oxidation and as a function of potential. In particular, the question of stability of the disulfide bond, and whether irreversible breakage of this bond to form Hg—S bonds occurs on adsorption, is of interest.

In connection with these studies of proteins (e.g., insulin, bovine serum albumin), we investigated the behavior of the amino acids cystine (RSSR) and cysteine (RSH), shown below in their zwitterionic forms. The electrochemistry of these substances at Hg has been studied, mainly by polarography, starting

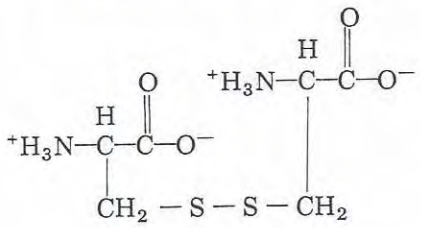

cystine (RSSR)

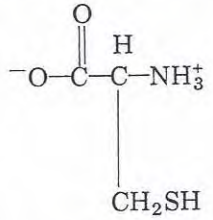

cysteine (RSH)

with the classical papers by Kolthoff and coworkers [5—8]. This work, as well as later papers [9—11], demonstrated that RSSR reduction is characterized by an adsorption "prewave" and a later diffusion-controlled reduction wave. The mechanism preferred for the prewave has generally involved the rapid (or kinetically controlled) reaction of RSSR with Hg, leading to breakage of the disulfide bond and production of mercuric cysteinate, which is the species reduced. This reaction with mercury thus accounted for the catalysis of the reduction at a mercury electrode compared with the irreversibility observed with Pt or Au electrodes [12—14]. However, a number of features (e.g., "double wave" formation) of the prewave and distinction between adsorbed RSSR and mercuric (or mercurous) cysteinate have not been elucidated. Moreover, the limited time window of even a slow dropping mercury electrode prevented studies of very low concentrations, where diffusion of reactant to the electrode surface does not give an appreciable accumulation of adsorbed species during the drop life. Since the nature of the interaction of the disulfide bond with the Hg surface is important in understanding the electrochemical behavior of proteins, we investigated the electrochemistry of RSSR and RSH at a hanging mercury drop electrode (HMDE) over a wide concentration range and at several pH's. In this study we conclude that the bond-breaking reaction between RSSR and Hg is slow and propose a mechanism for the reduction of RSSR and oxidation of RSH at Hg.

The various stages of protonation of RSSR, RSH, and $Hg(RS)_2$ were calculated using reported thermodynamic data [7,8,15] for the different pH's of

TABLE 1

Distribution of species at various pH's

pH	Cystine			Cysteine			Mercury cysteinate		
	HRSSRH	—RSSRH	—RSSR—	HRSH	—RSH	—RS—	$Hg(RSH)_2$	$Hg(RSH)(RS)^-$	$Hg(RS)_2^{2-}$
6.0	0.986	0.014	—	0.995	0.005	—	0.926	0.073	—
7.4	0.738	0.261	9×10^{-4}	0.896	0.103	8×10^{-5}	0.334	0.665	0.005
9.3	—	0.759	0.241	0.09	0.852	0.05	0.01	0.875	0.114
10.5	—	0.183	0.815	0.003	0.503	0.493	—	0.524	0.476

interest in this study; complete results and details are given in ref. 16. With the uncharged form of cystine written as HRSSRH, that of cysteine as HRSH, and that of mercuric cysteinate as $Hg(HRS)_2$, the calculated relative amounts of the various species at the pH's of the experiments in this work are shown in Table 1. Throughout the paper RSSR will be used as the abbreviation for cystine, RSH for cysteine, and $Hg(RS)_2$ for mercuric cysteinate for all forms present at the given pH.

EXPERIMENTAL

Chemicals

Water, triply distilled from alkaline permanganate solution, was used to prepare the aqueous solutions. The buffer solution and supporting electrolyte was 0.1 *M* phosphate, pH 7.4. Buffer solutions were prepared from equimolar amounts of Baker Analyzed Reagent $Na_2HPO_4 \cdot 12\ H_2O$ and Allied Chemical Reagent grade $NaH_2PO_4 \cdot H_2O$; this solution was adjusted to pH 7.4 by addition of 1 *M* KOH, made from Fisher Scientific (Certified ACS) pellets. Buffer solutions of pH 9.3 or higher were prepared from ammonium chloride (Matheson, Coleman and Bell, Reagent) and ammonia (Baker analyzed reagent). The mercury used for the hanging mercury drop electrode and the stirred mercury pool was triply distilled. Pre-purified nitrogen, passed over hot copper and then through distilled water to saturate it, was used to degas the system. L-Cystine and L-cysteine monohydrochloride monohydrate were used as obtained from Nutritional Biochemicals Corporation. In the one experiment run in liquid ammonia, the preparation and procedures followed previous practices of our laboratory utilizing vacuum line techniques [17].

Apparatus and procedure

The cell used for electrochemical studies is shown in Fig. 1. The working electrode for the coulometric experiment in this cell was a mercury pool of volume 25 to 30 ml (area, 7.6 cm^2), stirred by a Teflon-coated stirring bar immersed in the mercury. The auxiliary compartment contained 0.1 *M* NaCl and 0.1 *M* phosphate buffer; the auxiliary electrode was a silver wire. The reference electrode was a saturated calomel electrode (SCE) with a KNO_3-agar salt bridge. The SCE was separated from the working compartment by a glass sleeve with a medium porosity frit to prevent leakage of chloride into the working compartment. A Brinkman hanging mercury drop electrode (HMDE) was used; the drop area was 0.0267 cm^2 in all experiments. The solution volume was typically 18 ml.

Solutions and samples were degassed at least $\frac{1}{2}$ h before contact with mercury and commencement of electrochemical experiments. Nitrogen was passed over the solution during the experiments.

All cyclic voltammetric and coulometry experiments were performed with

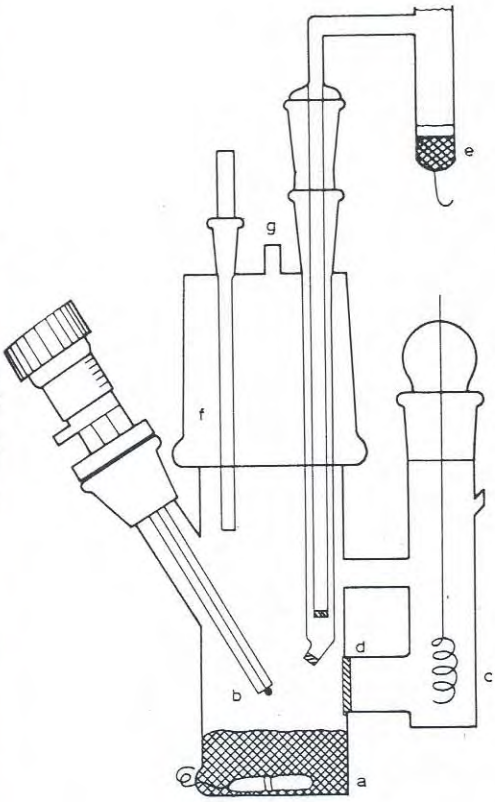

Fig. 1. Coulometry cell. (a) Mercury pool electrode — 25 ml, 7.6 cm^2; (b) hanging mercury drop probe electrode; (c) Ag auxiliary electrode and electrode compartment; (d) fritted sleeve for the reference electrode; (e) saturated calomel reference electrode with agar bridge; (f) nitrogen inlet; (g) septum.

a Model 170 Electrochemistry System (Princeton Applied Research Corporation, Princeton, N.J.). For scan rates faster than 500 mV s^{-1}, the i—E curves were recorded on a Tektronix Type 564 Storage Oscilloscope. Details of the experimental procedures and complete listings of experimental data are available [16].

RESULTS

Cyclic voltammetry of cystine (RSSR)

Typical cyclic voltammograms (c.v.) for cystine solutions at pH 7.4 are shown in Fig. 2. In these experiments a fresh mercury drop from the HMDE was pre-equilibrated in a stirred solution of RSSR for 1 min at open circuit (where the open circuit potential was about —0.32 V vs. SCE). Experiments

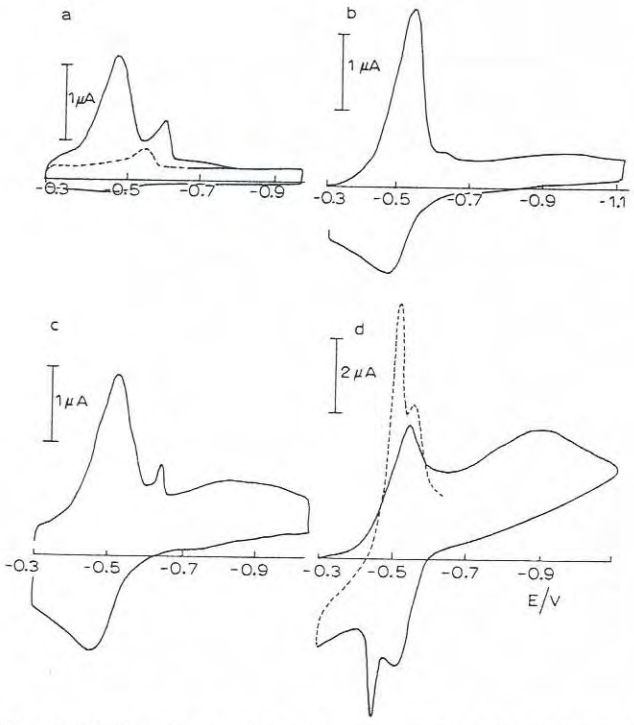

Fig. 2. Cyclic voltammetry of cystine at pH 7.4. The HMDE was pre-equilibrated in stirred solution for 1 min; the scan rate was 200 mV s^{-1} and the RSSR concentration was (a) 10^{-6} M; (b) 5×10^{-5} M; (c) 9×10^{-5} M; (d) 4.6×10^{-4} M.

were performed with RSSR concentrations of 1 μM to 0.46 mM. At low concentrations (Fig. 2a—c) the reduction showed a rather symmetrical wave at —0.53 V characteristic of an adsorbed reactant. The peak current, i_{pc}, for this wave was directly proportional to scan rate, v, for v's of 0.02 to 20 V s^{-1} (Fig. 3a) and the integrated area under the peak was 41 ± 2 μC cm^{-2} for all of the concentrations. Upon reversal of the scan after the first reduction wave an anodic wave at —0.47 V with a shape corresponding to that of a diffusing species was observed. The peak current for this wave, i_{pa}, was linear with $v^{1/2}$ (Fig. 3b). At RSSR concentrations above about 0.4 mM the behavior changed somewhat (Fig. 2d). While the characteristics of the first scan reduction waves were unchanged, upon reversal in addition to the diffusion-controlled oxidation wave a symmetrically shaped current "spike" appeared at more positive potentials. Upon reversal following this anodic scan the second reduction scan showed a symmetrical reduction "spike" at —0.515 V in addition to the first-scan reduction wave. However, at scan rates above 5 V s^{-1}, the symmetrical oxidation and reduction current spikes were not observed, and the reduction and oxidation waves had the same respective adsorption and diffusion pr per-

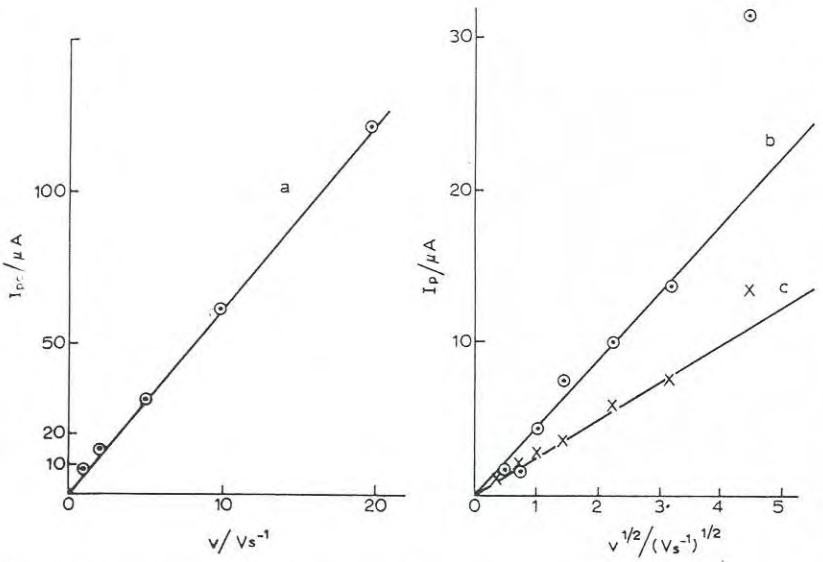

Fig. 3. Dependencies of peak currents (i_p) on scan rate (v) for various cyclic voltammetric peaks for a 0.4 m*M* cystine solution, pH 7.4, at HMDE. (a) i_{pc} vs. v for prewave (E_{pc} = —0.53 V); (b) i_{pa} vs. $v^{1/2}$ for anodic wave (E_{pa} = —0.47 V); (c) i_{pc} vs. $v^{1/2}$ for cathodic wave (E_{pc} = —0.9 V).

ties they possessed at lower concentrations. When the anodic current spike (E_{pa} — 0.455 V) was observed, the diffusion-controlled oxidation wave occurred at an E_{pa} of —0.515 V, and the reduction peak current on the second scan shifted from an E_{pc} of —0.535 to an E_{pc} of —0.555 V. This peak shift was observed even at high scan rates where the adsorption current spikes were not observed. The effect of changing scan rate on the shape of the cyclic voltammograms is shown in Fig. 4. Note that the current spikes disappear at higher scan rates, with the anodic spike disappearing before the cathodic one. The peak shapes and potentials and the integrated current were independent of pre-equilibration time (up to 5 min) and potential (from —0.3 to —1.3 V).

In addition to the adsorption reduction wave a second reduction wave occurs at —0.9 V. The i_p for this wave varied with $v^{1/2}$ and concentration and corresponds to diffusion-controlled reduction of dissolved RSSR. In results described later, a similar diffusion-controlled wave is observed for the reduction of RSSR in liquid ammonia on a gold electrode. Gold or platinum electrode experiments at potentials of this wave could not be performed for the aqueous buffer because of the occurrence of background reduction.

The results are consistent with the first wave processes consisting of the reduction of an adsorbed species to produce a nonadsorbed reduced form which is oxidizable upon scan reversal. At higher concentrations an adsorbed reduced form occurs which is oxidized to a new adsorbed oxidized form, thus producing the oxidation and reduction current "spikes" which are superim-

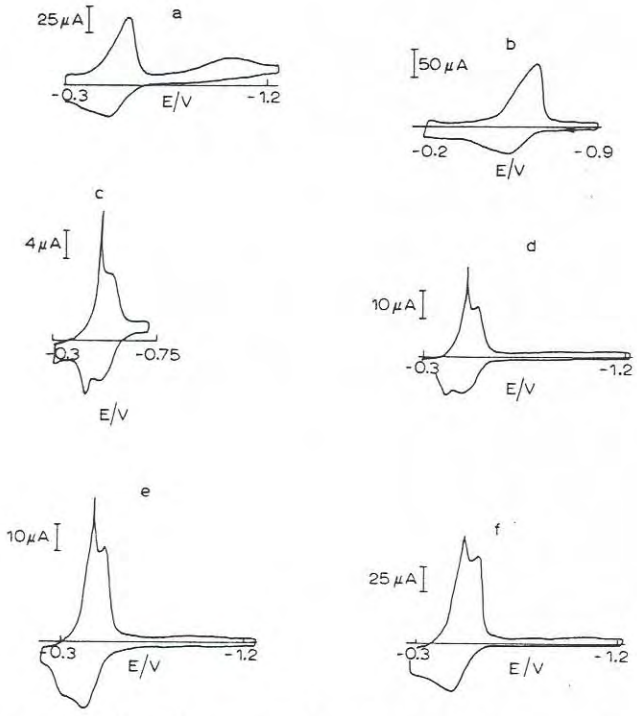

Fig. 4. Cyclic voltammetry of a 4.6×10^{-4} *M* cystine solution at different scan rates at HMDE in pH 7.4 buffer. (a) First scan, 5 V s^{-1}; steady state scans at (b) 10 V s^{-1}; (c) 0.5 V s^{-1}; (d) 1 V s^{-1}; (e) 2 V s^{-1}; (f) 5 V s^{-1}. The first reduction scans at all scan rates showed only the single reduction peak.

posed on the low concentration waves. The nature of the species involved was investigated further by studying the electrochemical oxidation of cysteine (RSH).

Cyclic voltammetry of cysteine (RSH)

Typical cyclic voltammograms of cysteine *(RSH)* at several concentrations in pH 7.4 buffer following pre-equilibration of a fresh mercury drop in stirred solution for 1 min at a potential of —0.65 V are shown in Fig. 5. For RSH concentrations up to 0.1 m*M* and scan rates of 0.2 V s^{-1}, only a single anodic wave characteristic of a diffusing species is observed. The i_{pa} of this wave varied linearly with concentration, c, and $v^{1/2}$. The reduction peak following scan reversal at —0.30 V was a symmetrical adsorption peak (see Fig. 5b), with i_{pc} proportional to v. A plot of the integrated reduction peak current vs. c is shown in Fig. 6. These results were independent of time for pre-equilibration of the mercury drop at —0.65 V for times of 10 s to 2 min. For an RSH concentration of 0.3 m*M* the behavior depended upon v. At scan rates above

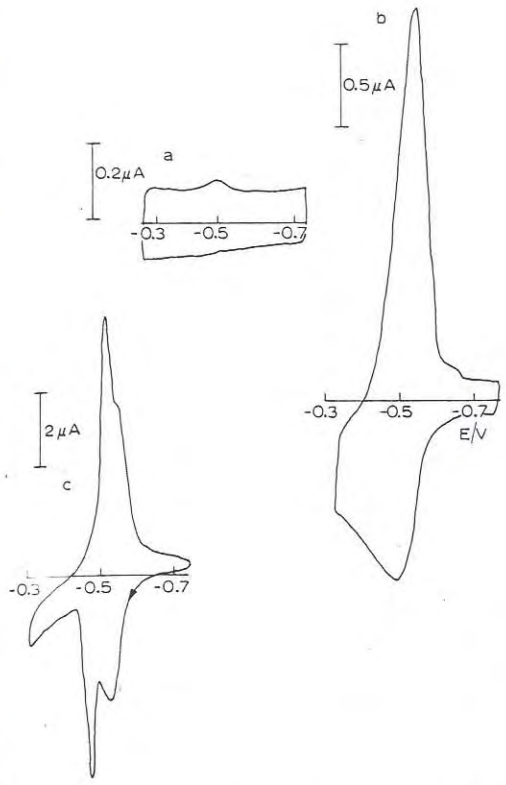

Fig. 5. Cyclic voltammetry of cysteine at pH 7.4. The HMDE was pre-equilibrated in stirred solution for 1 min while held at —0.65 V. The RSH concentrations were (a) 9.0×10^{-7} *M*; (b) 9×10^{-5} *M*; (c) 3×10^{-4} *M*.

5 V s^{-1}, the anodic and cathodic waves were generally the same as those at lower concentration. At lower scan rates (Fig. 5c) two anodic waves appeared, with the diffusion wave shifted from —0.47 to —0.52 V and a sharp symmetrical current spike appearing at —0.455 V; the anodic current decreased abruptly after this current spike. Upon scan reversal past this spike a cathodic spike at —0.515 V appeared, with the broader cathodic adsorption wave occurring at —0.555 V. If the anodic scan was reversed before the anodic current spike (e.g., at —0.46 V), the cathodic current spike at —0.515 V was not observed. The linear variation of i_{pa} with c observed for concentrations up to ca. 0.3 m*M* no longer holds at higher concentrations, where the i_{pa} vs. c curve levels off. Thus for a 0.32 m*M* solution, i_{pa} = 3.1 μA, while for 0.5 m*M*, i_{pa} = 3.4 μA. The cyclic voltammogram for an RSH concentration of 0.5 m*M* was essentially the same as that of the 0.3 m*M* solution. At these concentrations the integrated reduction current reached its maximum value of 80 ± 2 μC cm^{-2}.

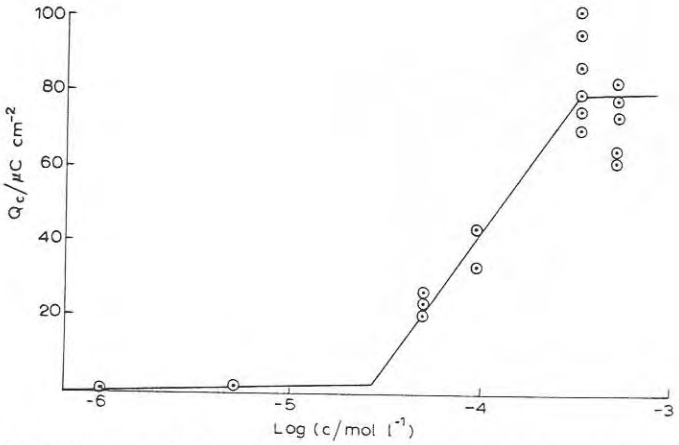

Fig. 6. Integrated reduction current following cysteine cyclic voltammetric oxidation wave vs. concentration at the HMDE.

Coulometric reduction of RSSR

To obtain more information about the reaction path and especially about the extent of the direct reaction between mercury and RSSR to form an organomercury intermediate, coulometric reduction of a 0.44 m*M* RSSR solution in pH 7.4 buffer at a stirred mercury pool was carried out. The solution composition was monitored with time and stage of electrolysis by cyclic voltammetry at an HMDE located above the pool (Fig. 1). Immediately upon introduction of the RSSR and after stirring over the mercury pool at open circuit for 10 to 15 min, the voltammogram was the same as that previously described (Fig. 2d). After stirring at open circuit for 15 to 30 min, however, the cyclic voltammogram showed the double peak pattern on the first reduction sweep (Fig. 7a). This double peak was seen only on the first scan, however; subsequent scans taken shortly after the first showed the single peak reduction. The solution after different times and at different stages of the electrolysis was also tested for the presence of mercuric ion using both the cuprous iodide (formation of orange Cu_2HgI_4) [18] and H_2S (formation of black HgS) [19] spot tests. Both of these tests were shown to give positive indications for mercuric cysteinate at concentrations down to 10^{-6} *M* in the pH 7.4 buffer. A control, in which the deaerated buffer was stirred over the mercury pool, did not give a positive Hg(II) test. The cystine solution which was stirred over a mercury pool for 15—30 min gave a slight positive test for Hg(II); the intensity of the spot corresponded roughly to a 10^{-6} *M* $Hg(RS)_2$ solution. These results are consistent with the relatively slow formation of an organomercury intermediate with stirring by direct reaction of RSSR at the large area mercury pool (for simplicity and consistency with previous work, we will refer to this intermediate as mercuric cysteinate, $Hg(RS)_2$, although

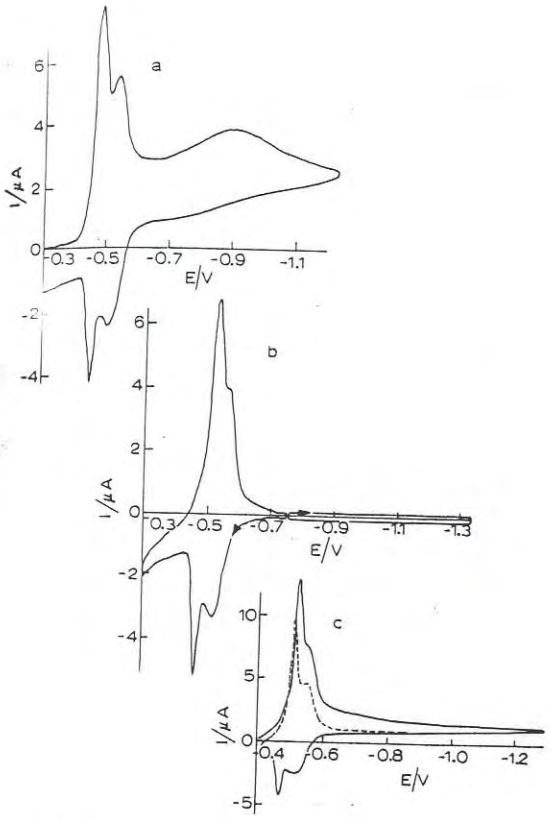

Fig. 7. Cyclic voltammetry at HMDE at different stages of the coulometric reduction of 0.46 m*M* cystine at a stirred mercury pool at pH 7.4; scan rate, 200 mV s^{-1}. (a) Cystine prestirred over the mercury pool for 1 h; (b) after cystine reduced at —0.750 V; (c) after reoxidation at —0.40 V.

it may contain Hg(I) as well as Hg(II) [11]). This species can then dissolve and readsorb at the HMDE to form the reductive current spike. The reaction rate between RSSR and Hg is apparently sufficiently slow at low RSSR concentrations that this wave does not appear in solutions only containing a HMDE. Note that the diffusion controlled RSSR reduction wave is still present at essentially its original height on the HMDE scan in Fig. 7a, so that only small amounts of RSSR are converted to $Hg(RS)_2$ even after 1 h.

Coulometric reduction of the RSSR at the mercury pool at —0.75 V showed an n_{app} = 1.97 based on the initial RSSR concentration. After this reduction the HMDE scan (Fig. 7b) towards negative potentials shows that the diffusion-controlled reduction wave has disappeared. The oxidative scan and reversal matched that of a 0.3 m*M* solution of RSH. The integrated area of the reduction peaks corresponded to 80 μC cm^{-2} and a spot test showed no Hg(II) in solution. Coulometric reoxidation at the pool at —0.40 V showed an n_{app} =

1.58, a strong positive spot test for Hg(II) and a cyclic voltammogram (Fig. 7c) in which the diffusion-controlled reduction wave was absent and the double peaks with adsorption spikes are apparent. Although the diffusion-controlled reduction peak at —0.9 V was absent, appreciable cathodic current was observed in the decaying tail of the adsorption reduction peaks (at —0.6 to —0.7 V), suggesting continued reduction of a nonadsorbed species diffusing to the HMDE. After reduction of this solution at —0.75 V, a negative spot test for Hg(II) resulted.

Reduction of RSSR in liquid ammonia

Several experiments were performed in liquid ammonia solutions to allow comparison of the behavior at a mercury electrode to that at solid electrodes at potentials unavailable in aqueous solutions. The apparatus and methodology for these experiments followed previous practice [17]. Typical results for the reduction of a 3 m*M* solution of the dipotassium salt of cystine at Hg and Au electrodes are shown in Fig. 8a and b. While the diffusion-controlled wave at about —1.1 V vs. Ag/Ag^+ was observed at Hg, Au, and Pt, the reversible pair at —0.5 V only appeared with the Hg electrode. Coulometric reduction of the solution at a Pt foil electrode at potentials of the diffusion-controlled wave

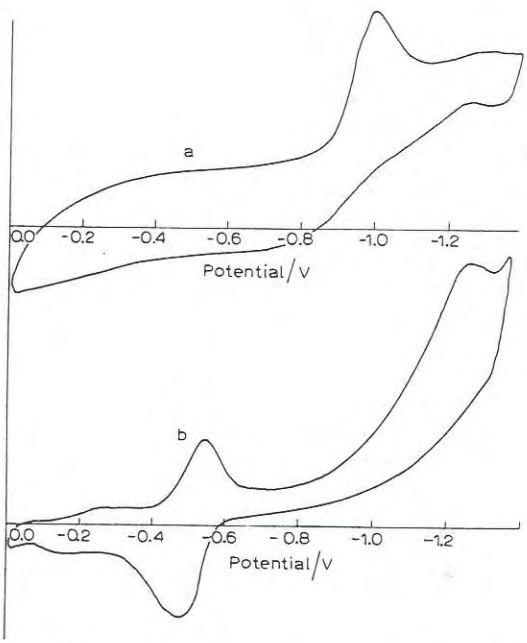

Fig. 8. Cyclic voltammetry in liquid ammonia + 0.1 *M* KI; v = 200 mV s^{-1}. (a) Cystine-Au electrode; (b) cystine-HMDE. Potential is vs. the Ag/Ag^+ electrode.

showed an $n_{app} = 1.4$. Following the reduction no oxidation or reduction waves were observed at the Pt electrode within the available range of potentials of liquid ammonia. However, at a mercury electrode the reduced product showed a large oxidation current spike which decreased upon addition of acetic acid.

pH dependence in aqueous solutions

At pH 6.0 both RSSR and RSH are essentially completely in their fully protonated forms. The cyclic voltammetric behavior at this pH for both cystine and cysteine was the same as that at pH 7.4, except that the adsorption waves were displaced towards more positive potentials by an average of 53 mV/pH unit. At pH 9.3 the mono-deprotonated forms of RSSR and RSH predominate. For RSH at a concentration of 0.85 m*M* and at slow scan rates (e.g., v of 20 mV s^{-1}) an oxidation wave at −0.49 V and reduction wave on reversal at −0.54 V appear. At low scan rates i_{pa} and i_{pc} vary as $v^{1/2}$ and i_{pc}/i_{pa} are near one. Thus diffusion-controlled oxidation of RSH to a solution species is suggested. At higher scan rates (1 to 10 V s^{-1}) the oxidation and reduction waves show definite double peaks, i_{pc} and i_{pa} show large positive deviations from the $v^{1/2}$ correlation, and i_{pc}/i_{pa} is larger than one (reaching 1.86 at 10 V s^{-1}). Very similar behavior is found for RSH at pH's 10 and 11.3, where appreciable amounts of the dideprotonated form exist, except that the waves are not resolved into double peaks. The results suggest that both adsorbed and solution phase RSH (and RSSR) undergo electrochemical reactions. Current "spikes" are never seen at these alkaline pH's. In this range the shift of E_{pa} and E_{pc} with pH was about 39 mV/pH unit. The reduction of a 0.48 m*M* solution of RSSR at pH 9.3 shows a cyclic voltammetric wave at −0.57 V with i_{pc} varying with v and an integrated area of 35 μC cm^{-2}. The shape of the oxidation wave on reversal depends upon the reversal potential, but appears to be composed of the two waves observed on RSH oxidation. At a concentration of 0.9 m*M* both reduction and oxidation waves were primarily diffusion-controlled.

Effect of addition of sodium dodecyl sulfate (SDS)

SDS, a detergent which shows strong adsorption at the Hg-water interface, was added to RSSR and RSH solutions to study its effect on the cyclic voltammetric behavior; previous experiments on the effect of surface-active agents in this system have been reported [8,20]. Typical results are shown in Fig. 9. In a pH 7.4 buffer, SDS alone shows symmetrical reversible current peaks characteristic of capacitance changes involved with rearrangement of adsorbed species [21]. When the solution contained 0.2 m*M* RSSR, the wave attributed to adsorbed RSSR at −0.5 V and its reversal wave were absent, although the background current levels in the presence of RSSR were somewhat larger than in its absence (Fig. 9b). When the potential was scanned

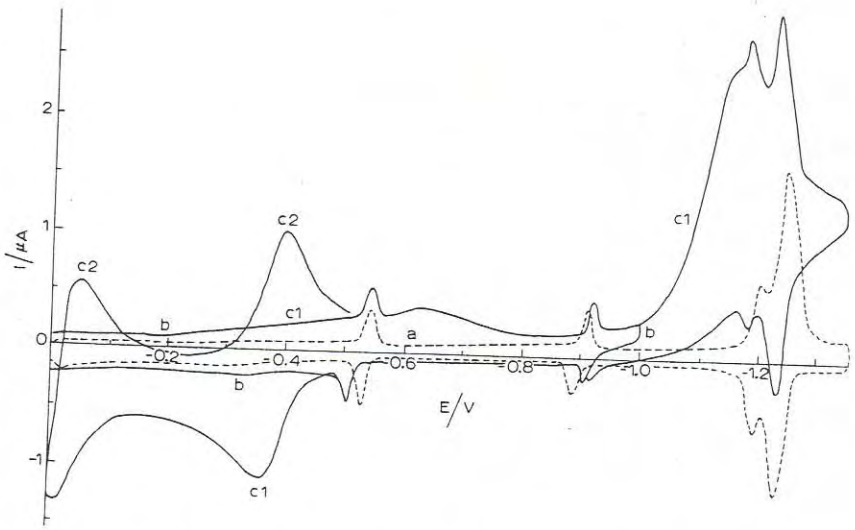

Fig. 9. Cyclic voltammetry of 0.2 *M* SDS, pH 7.4, scan rate 200 mV s^{-1}. (a) 0.2 SDS alone; (b) 0.2 *M* SDS, 0.2 m*M* cystine, scan reversed at −1.0 V; (c) 0.2 *M* SDS, 0.2 m*M* cystine, scan reversed at −1.35 V.

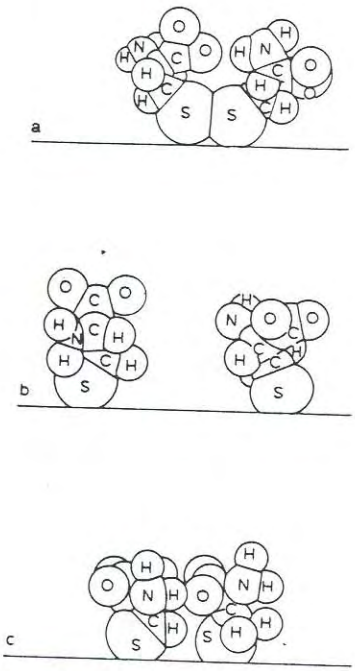

Fig. 10. Nature of adsorbed species under different conditions. (a) RSSR; (b) $Hg(RS)_2$; (c) $Hg(RS)_2$, compact film.

beyond −1.0 V (Fig. 9c), a diffusion-controlled reduction wave appeared at about −1.2 V. On reversal at −1.3 V a new pair of diffusion-controlled waves (determined by the i_p–$v^{1/2}$ dependence) appeared: an anodic wave at −0.36 V and a corresponding cathodic wave on reversal at −0.40 V. This couple is the same as that found for the oxidation and reduction of 0.35 m*M* RSH in the presence of 0.2 *M* SDS on a scan from −1.0 V to −0.2 V and reversal. The current "spikes" were absent in the presence of SDS. Although the details of the mechanism of the reduction in the presence of SDS were not probed further, the results can be explained in terms of SDS adsorption blocking the adsorption of the RSSR and RSH species, thus eliminating the adsorption waves, but allowing electron transfer to solution phase RSSR and RSH. The existence of the diffusion-controlled reduction wave at −0.40 V following oxidation of RSH (or reduction of RSSR, then oxidation and scan reversal), where this wave does not appear in the original RSSR solution, shows the formation of an oxidized form of RSH which is not dissolved RSSR.

DISCUSSION

The following mechanism at pH 7.4 emerges from the reported results. For cysteine (RSH), the species RSH is not strongly adsorbed, and its oxidation leads to an adsorbed species, usually considered to be mercuric cysteinate [$Hg(RS)_2$]. Thus the anodic (−0.47 V) and cathodic (−0.52 V) pair that appears at concentrations below 0.3 m*M* can be represented by

$$2(RSH)_{soln} + Hg \rightleftharpoons [Hg(RS)_2]_{ads} + 2\,H^+ + 2\,e \qquad (1)$$

At higher concentrations of RSH (e.g., 0.3 and 0.6 m*M*), anodic and cathodic current spikes appear in addition to the above waves (with a slight shift in potentials). This can be ascribed to the attainment of monolayer coverage of the $Hg(RS)_2$ species and the formation of a tight "film" when lateral interactions between the adsorbed molecules occur. The nature of this film formation will be discussed later. The maximum integrated reduction current, corresponding to adsorbed $Hg(RS)_2$, is 80 $\mu C\ cm^{-2}$. Thus the RSH results can best be described as mercury oxidation to form adsorbed mercuric cysteinate.

The cystine (RSSR) results suggest that the first scan reduction wave corresponds to the reduction of adsorbed RSSR with breakage of the disulfide linkage and formation of dissolved RSH (0.54 V):

$$(RSSR)_{ads} + 2\,H^+ + 2\,H^+ + 2\,e \rightarrow 2(RSH)_{soln} \qquad (2)$$

The direct reaction between mercury and RSSR to form mercuric cysteinate does *not* occur to an appreciable extent in the cyclic voltammetry experiments and even when an RSSR solution is stirred over a mercury pool for up to 15 min. The amount of $(RSSR)_{ads}$ corresponds to 41 $\mu C\ cm^{-2}$. If a model of RSSR is constructed and the area that it occupies when the disulfide bond is oriented on the electrode surface is calculated, a monolayer coverage corresponding to 2.3×10^{-10} mol cm^{-2} or 44 $\mu C\ cm^{-2}$ ($n = 2$) is predicted. Upon

scan reversal the dissolved RSH now is oxidized by the reaction sequence shown in (1). The $Hg(RS)_2$ species is apparently more strongly adsorbed than the RSSR, so that subsequent scans show the typical RSH behavior, along with the current spikes at higher concentrations. Dissolved RSSR is reduced to RSH at −0.9 V:

$$(RSSR)_{soln} + 2\,H^+ + 2\,e \rightarrow 2(RSH)_{soln} \qquad (3)$$

The relative strength of adsorption decreases in the order $Hg(RS)_2 > RSSR >> RSH$. Justification of the proposed mechanism and further details will now be discussed.

The mechanism is based on the adsorption of RSSR, its lack of reaction with mercury, the formation of adsorbed $Hg(RS)_2$ on oxidation of nonadsorbed RSH, and film formation or adsorbed layer reorganization of $Hg(RS)_2$.

Adsorption of RSSR

The reduction wave at −0.54 V shows an i_{pc} proportional to v and an integrated area independent of concentration and in good agreement with that calculated, assuming monolayer coverage by RSSR. For a 10^{-6} *M* RSSR solution only a very small wave is observed at a fresh mercury drop. However, on standing or after stirring for 1 min, the well-developed symmetrical wave appears. Thus at low concentrations, diffusion limits the supply of RSSR to the electrode [22], but with stirring, close to monolayer coverage is attained. At concentrations above 10^{-5} *M* the integrated reduction currents were independent of pre-equilibration time. Adsorption of the surface-active agent SDS eliminates the RSSR adsorption wave by blocking the surface for the adsorption of RSSR. Similar effects of surface-active agents on the reduction of RSSR have been noted previously [8,20].

Lack of significant reaction between mercury and RSSR

Using the thermodynamic data for the ionization constants of RSSR and RSH [15], the formation constants of mercuric cysteinate species [7], and the redox potential for Hg/Hg(II) and RSSR/RSH [8], we calculated the extent of formation of mercuric cysteinate by reaction of Hg and RSSR as a function of pH and RSSR concentration; details and complete results are given elsewhere [16]. The maximum extent of formation of $Hg(RS)_2$ occurred at pH 9 where the ratio of $Hg(RS)_2$ to RSSR species was 0.62%. At a pH of 7.5 for a total RSSR concentration of 4×10^{-4} *M*, only 0.48% would be converted to mercuric cysteinate species. This number essentially agrees with the value of Kolthoff et al. [8] *. Thus the local concentration of $Hg(RS)_2$ near

* Our calculated values are based on thermodynamic data obtained from polarographic measurements ignoring the free energy of adsorption of RSSR [8]. As Nygard [9] points out, the reported data for this system, obtained from measurements at a mercury electrode, may be in error.

the mercury drop, assuming immediate equilibrium, would be ca. 2×10^{-7} *M*, while at a 10^{-6} *M* RSSR concentration this would be ca. 5×10^{-9} *M*. It is unlikely that such concentrations would form a monolayer of adsorbed $Hg(RS)_2$. Moreover, the studies of RSH oxidation at concentrations of 3×10^{-4} *M* or higher and scan rates of 200 mV s^{-1} show that the reduction of $Hg(RS)_2$ is characterized by double adsorption peaks (the current spike and the adsorption peak) (Fig. 5c), so that this can be used as a test for the presence of $Hg(RS)_2$. This behavior is never seen for the first scan of a 4.6×10^{-4} *M* RSSR solution equilibrated with a HMDE for 10 s to 5 min at potentials of 0 to −0.4 V. The same single peak behavior with an integrated area of 41 μC cm^{-2} was always seen; the double peak only resulted following the anodic scan (Fig. 4d).

Finally, the results obtained with the stirred mercury pool are persuasive. Only after stirring for more than 15 min does the double peak behavior appear on the initial scan with the HMDE above the pool and is Hg(II) detected by a spot test. Even under these conditions, the diffusion-controlled peak for RSSR reduction ($E_{pc} = -0.90$ V) was essentially unchanged in magnitude, so that extensive conversion of RSSR to $Hg(RS)_2$ did not occur. Moreover, at pH 9.3 under conditions where RSH oxidation *and* the reversal reduction show diffusion-controlled behavior, RSSR shows an adsorption peak on the initial reduction scan.

It is possible that $Hg(RS)_2$ is an intermediate in the reduction of adsorbed RSSR, but the state of the surface species existing prior to the reduction scan is probably better thought of as $(RSSR)_{ads}$ with its disulfide bond intact. While previous studies [8,9] of cystine involving polarography or linear scan voltammetry at a dropping mercury electrode have suggested, because of the nature of the dependence of the current on column height or drop time, that the current at the adsorption wave of RSSR was a kinetically controlled one, the kinetics involved during the 3.5 to 7 s drop life may have involved RSSR adsorption rather than reaction with mercury. While Kolthoff et al. [8] found that the prewave height was almost proportional to RSSR concentration for 3.5 s drop times, we have found that with 1-min equilibration times in stirred solution the integrated peak height was independent of concentration. Moreover, the temperature coefficient of the prewave [8] was smaller than that expected of a kinetic process.

Formation of adsorbed $Hg(RS)_2$ by oxidation of dissolved RSH

The i_{pa} for RSH oxidation varied with $v^{1/2}$ (even at concentrations where the current spike was observed) and was proportional to the RSH concentration between 10^{-5} and 10^{-4} *M*. Moreover, i_{pc} was independent of the time for which the HMDE was equilibrated with the solution before the anodic scan and the oxidation wave was observed in the presence of SDS. These all demonstrate that dissolved RSH was the species oxidized. The i_{pc} on scan reversal for concentrations below 3×10^{-4} *M* was proportional to v; above this con-

centration the occurrence of the cathodic current spike made measurements of this wave height uncertain. The integrated cathodic current equaled that of the anodic current, reaching a maximum of 80 μC cm^{-2}. The experiment in which $Hg(RS)_2$ was produced by stirring an RSSR solution over a mercury pool for 1 h to produce a solution containing about 4×10^{-4} M RSSR and 10^{-6} M $Hg(RS)_2$ and observation of the cyclic voltammetry at the HMDE demonstrates that $Hg(RS)_2$ is more strongly adsorbed than RSSR. On the first scan the behavior is that of monolayer of $Hg(RS)_2$ (Fig. 7a) even with the much larger concentrations of RSSR. Subsequent scans taken immediately afterwards were those attributable to RSSR, since the RSH formed during reduction was not adsorbed and RSSR adsorption could then occur.

Film formation

At concentrations of RSH where monolayer coverage of $Hg(RS)_2$ is attained, current spikes appear on the anodic and cathodic scans (Figs. 5 and 6). An explanation for these current spikes involves the formation of a "tight" or complete monolayer (or compact film). Such sharp changes in coverage for small concentration changes in solution (i.e., adsorption isotherm discontinuities or two-dimensional crystallization) have been shown [23,24] to occur when there are strong attractive interactions between the adsorbed molecules. While we do not know the structure of the film, some possible arrangements based on molecular models of the adsorbed molecules are shown in Fig. 10. The adsorbed RSSR with the disulfide linkage at the mercury surface would show the lowest coverage. The $Hg(RS)_2$ species involves breaking the disulfide bond, which allows closer packing of the molecules. The compact film would occur when interactions between the RS^- species cause a tight packing or "crystallization" on the surface. These interactions could involve hydrogen bonding between the $-NH_2$ group of one molecule and the $-COOH$ group on an adjacent one; models with the S atoms oriented on a plane with this type of intermolecular bonding show this arrangement is possible sterically. This tight packing can account for the higher coverage of the complete $Hg(RS)_2$ film (80 μC cm^{-2}) as compared to that of RSSR (40 μC cm^{-2}). The current in the spikes is probably nonfaradaic, arising from the sharp change in double layer capacitance upon compact film formation (surface structure reorganization and desorption of water), but may also include some faradaic current. The leveling off of the i_{pa} vs. c curve at concentrations where the compact film forms suggests that diffusing RSH cannot penetrate this film, although diffusion-controlled oxidation of RSH continues during build-up of adsorbed $Hg(RS)_2$ until this point. The low value of n_{app} upon coulometric oxidation of RSH formed during reduction of RSSR may be caused by such electrode blockage by the compact film. The fact that the current spikes are not observed at all at faster scan rates, or that the cathodic spike is sometimes observed during oxidation of RSH when the anodic spike is absent or is very small (Fig. 4) suggests that some time is required for the compact film to form.

Based on the cyclic voltammetric experiments, the rate constant for compact film formation is of the order of 0.1 s^{-1}. Finally, the lack of current spikes at pH's of 9.3 and above, where deprotonated forms of the RSSR, RSH, and $Hg(RS)_2$ predominate, suggests that intermolecular hydrogen bonding is important in compact film formation.

ACKNOWLEDGMENTS

The support of the Robert A. Welch Foundation (F-079) and the National Science Foundation (CHE 71-03344) is gratefully acknowledged.

REFERENCES

1 P.R. Moses, L. Wier and R.W. Murray, Anal. Chem., 47 (1975) 1882.
2 B.F. Watkins, J.R. Behling, E. Kariv and L.L. Miller, J. Amer. Chem. Soc., 97 (1975) 3549.
3 N.R. Armstrong, A.V.C. Lin, M. Fujihira and T. Kuwana, Anal. Chem., 48 (1976) 741.
4 R.F. Lane and A.T. Hubbard, J. Phys. Chem., 77 (1973) 1401.
5 I.M. Kolthoff and C. Barnum, J. Amer. Chem. Soc., 62 (1940) 3061.
6 I.M. Kolthoff and C. Barnum, J. Amer. Chem. Soc., 63 (1941) 520.
7 W. Stricks and I.M. Kolthoff, J. Amer. Chem. Soc., 75 (1953) 5673.
8 I.M. Kolthoff, W. Stricks and N. Tanaka, J. Amer. Chem. Soc., 77 (1955) 4739.
9 B. Nygard, Acta Universitatis Upsaliensis, 104, Uppsala, 1967; B. Persson and B. Nygard, J. Electroanal. Chem., 56 (1974) 373 and references therein.
10 W. Lee, Biochem. J., 121 (1971) 563.
11 I.R. Miller and J. Teva, J. Electroanal. Chem., 36 (1972) 157.
12 J. Koryta and J. Pradac, J. Electroanal. Chem., 17 (1968) 177.
13 J. Koryta and J. Pradac, J. Electroanal. Chem., 17 (1968) 185.
14 D.G. Davis and E. Bianco, J. Electroanal. Chem., 12 (1966) 254.
15 H. Mahler and E. Cordes, Biological Chemistry, Harper and Row, New York, 1966, p. 10.
16 M.T. Stankovich, Ph.D. Dissertation, The University of Texas at Austin, 1975.
17 W.H. Smith and A.J. Bard, J. Amer. Chem. Soc., 97 (1975) 5203.
18 F. Feigl and V. Anger, Spot Tests in Inorganic Analysis, Elsevier, New York, 1972, p. 308.
19 D. Seyferth, J. Burlitch, R. Minasz, J. Yick-Pui-Mui, H. Simmons, A. Trieber and S. Dowd, J. Amer. Chem. Soc., 87 (1965) 4259.
20 I.M. Issa, A.A. El Samahy, R.M. Issa and Y.M. Temerik, Electrochim. Acta, 17 (1972) 1615.
21 E. Laviron and B. Riollet, Bull. Chem. Soc. Fr., (1968) 5077.
22 P. Delahay and I. Trachtenberg, J. Amer. Chem. Soc., 79 (1957) 2355.
23 M.J. Weaver and F.C. Anson, J. Electroanal. Chem., 60 (1975) 19.
24 C.M. Elliot and R.W. Murray, Anal. Chem., 48 (1976) 259.